ID 1299

LONG-TERM DURABILITY PERFORMANCE FOR ADVANCED HIGH TEMPERTURE POLYMER MATRIX COMPOSITES

Kazumi HIRANO
National Institute of Advanced Industrial Science and Technology (AIST), METI.
Namiki 1-2, Tsukuba-shi, Ibaraki-ken 305-8564, Japan

SUMMARY: The final goal of this research is to achieve through long-term and short-term tests under conditions simulating SST flight, development of associated predictive and accelerated test methods, and assessment of durability performances for design. The effects of open-hole, stress ratio and temperature on fatigue lives were investigated for both the screening of new composite materials and the determination of a baseline design allowable for ensuring the long-term structural integrity of primary structural components. This paper summarizes the open-hole fatigue strength characteristics for the interesting polymer matrix composite candidates in Japan Supersonic Research Program for 2nd Generation Supersonic Civil Transport. The test results show that there is a remarkable influence of stress ratio on open-hole fatigue strength characteristics, and fully reversed tension-compression (R= -1) fatigue lives are lowest as compared with tension-tension (R=0.05) and compression-compression (R=20) fatigue lives. There is also a unique relationship between normalized minimum stress by static open-hole compression strength σ_{min}/OHC and cycles to failure N_f regardless of test temperature.

KEYWORDS : Long-term Durability, High Temperature Polymer Matrix Composites, Open-hole Fatigue Strength, Normalized S-N Diagram, Stress Ratio, Elevated Temperature.

INTRODUCTION

One of critical technological issues to be solved for the realization of the supersonic transportation (SST) is how to ensure the long-term structural integrity of advanced polymer matrix composite system. This research has been conducted as a part of evaluating and predicting long-term durability performance of candidate composite and structures in Japan Supersonic Research Program for 2nd Generation Supersonic Civil Transport [1]. The final goal of this research is to achieve through long-term and short-term tests under conditions simulating SST flight, research and development of associated predictive and accelerated test methods, and assessment of durability performances for design.

Relatively little information is available on the long-term durability performance of high temperature thermosetting and thermoplastic polymer matrix composites, such as fatigue and creep as compared with conventional epoxy matrix composites. Generally, the greater short-term performance may not translate directly into improved performance under long-term loading conditions. Secondly, there are much differences in the initiation and propagation of damage in the interaction between damage modes and in the influence of fiber fracture on stiffness, residual tensile and compressive strength, and failure mode during long-term loading.

The objective of this paper is to investigate open-hole fatigue behavior and to compare the long-term durability performance between the interesting polymer matrix composite candidates. The effects of open-hole, stress ratio and test temperature on fatigue lives were summarized for both the screening of new composite materials and the determination of a baseline design allowable for ensuring the long-term structural integrity of primary structural components.

MATERIALS AND EXPERIMENTAL PROCEDURE

Materials and Test Specimens

The materials investigated in this study are carbon fiber reinforced, toughened bismaleimide (BMI), G40-800/5260, thermoplastic polyimide, IM600/PIXA-M and thermosetting polyimide, MR50K/PETI-5. Generally, the former bismaleimide resin has superior to the latter two polyimides in terms of composite fabrication. These materials were fabricated at KHI, FHI and MHI Co. Ltd, respectively. Main room-temperature mechanical and chemical properties[2] are summarized in Table 1. They were machined into specimens 160 mm long by 38.1 mm wide from the as-fabricated quasi-isotropic $[+45^0/0^0/-45^0/90^0]_{4s}$ stacking sequence panels. The mean panel thickness was ranging from 4.5 to 4.6 mm. The zero-degree direction coincides with the loading axis, and positive angles of ply orientation are measured clockwise from zero. A 6.35 mm hole was machined into the center of each specimen using a diamond core drill as shown in Fig. 1. The end tab material was approximately 3 mm thick glass epoxy bonded to the specimen using a general purpose epoxy. For the compression-compression fatigue testing at elevated temperature, the non-end tabs specimens were partially used with the unsupported length of 60 mm. All specimens were nondestructively inspected before testing to document machining defects. There was no biasing of damage development due to initial defects.

Table 1 Room temperature mechanical and chemical properties of panels

	G40-800/5260	IM600/PIXA-M	MR50K/PETI-5
OHT MPa	569	461	426
Tensile modulus GPa	NA	58.2	55.1
OHC MPa	385	309	317
Compressive modulus GPa	57.2	60	53.8
CAI (1500 in.lb/in.)	358	383	298
Tg ˚C	274	235	250

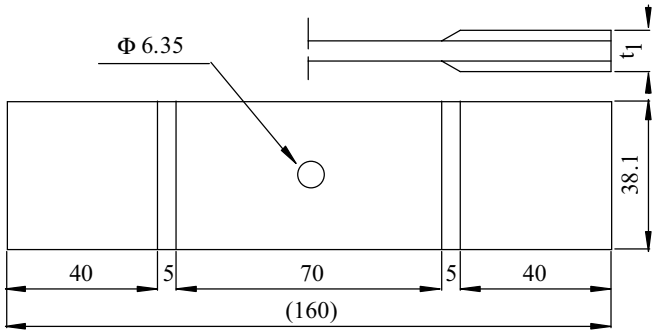

Fig. 1 Configuration and dimensions of test specimen

Experimental Procedure

RT/Dry open-hole fatigue tests were performed with load controlled-mode, sinusoidal wave-form, at a constant cyclic frequency of 5 Hz using the personal computer-controlled MTS materials testing system with environmental chamber (see Fig. 2) kept temperature at 23 ±1 ˚C and relative humidity at 50±2%. For both monotonic and cyclic loading, the specimens were also positioned in hydraulic grips with the alignment adjustable fixture. Stress ratio is changed from R=0.05 (tension-tension), R= -1 (fully reversed, tension-compression) to R=20 (compression-compression). Cyclic stress versus strain curves

were continuously measured by using extensometer (gauge length 25.4 mm) mounted on the specimen face, and monitored stiffness changes as a means of evaluating damage accumulation during fatigue loading.

HT/Dry open-hole compression-compression (R=20) fatigue tests were also performed using the non-tabs specimen under load controlled-mode with a sinusoidal waveform at a constant cyclic frequency of 5Hz at 149˚C for G40-800/5260 and 177˚C for both IM600/ PIXA-M and MR50K/PETI-5 in a dry environment. Laser optical microscope, TEM and soft X-ray radiograph examinations were also conducted at every fatigue damaged stages in order to examine fatigue damage initiation and propagation behavior from a root of initial circular hole.

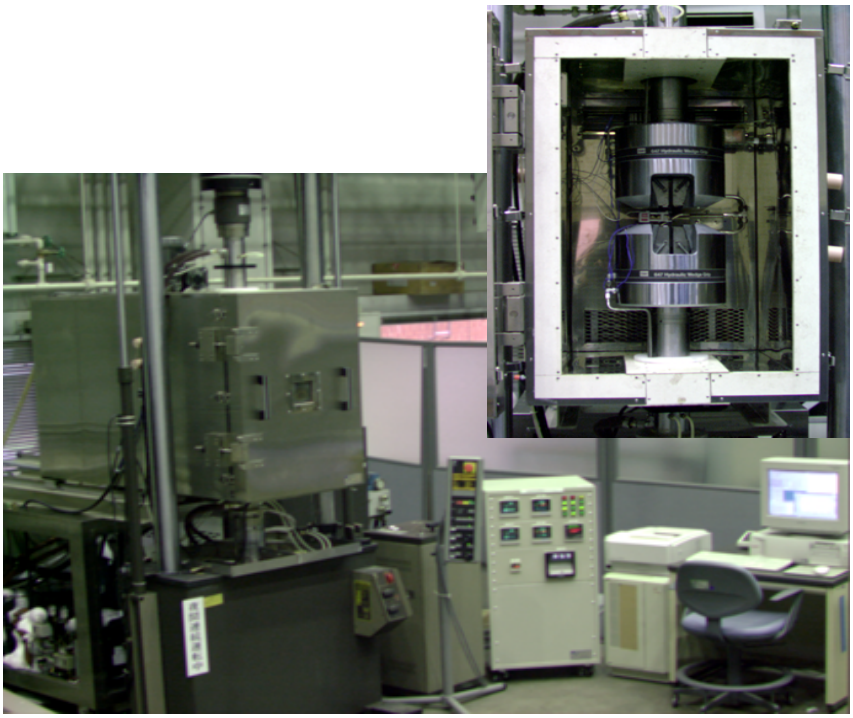

Fig. 2 Schematics of materials testing system with environmental chamber

RESULTS AND DISCUSSION

Open-hole Tension-tension Fatigue Behavior

Cyclic maximum and net stresses versus cycles to failure (σ_{max} , σ_{net} -N_f) relationships obtained at open-hole tension-tension fatigue tests are shown for both G40-800/5260 and IM600/PIXA-M in Figs. 3(a) and (b) in comparison with smooth specimen. It is not a little surprised that the σ_{net}- N_f plots fairly correspond to the exploration of σ_{max} - N_f relationships of smooth specimen especially at lower stress levels, in high-cycle region longer than 10^5 cycles, although there is a quite difference at higher stress levels. There is also a difference in a slope of S-N diagram depending on material properties. It should be noted here that there is little hole-sensitivity to the room temperature tension-tension fatigue behavior at high cycles region within the limits of this experiments regardless of materials. Soft X-ray radiograph examinations show that it is resulted from the reduction of stress concentration due to fatigue damage initiation and propagation at lower stress levels.

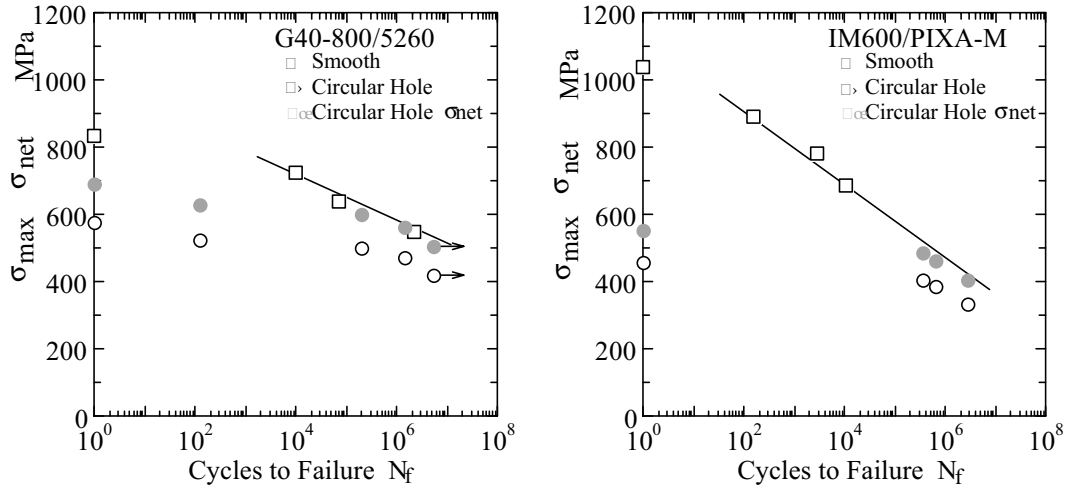

(a) G40-800/5260 (b) IM600/PIXA-M

Fig. 3 Comparisons of open-hole tension-tension fatigue behavior with smooth specimen

Open-hole Fatigue Strength Characteristics

Cycles-to-failure N_f are plotted against gross maximum and minimum stresses σ_{max} , σ_{min} at every stress ratio in Figs. 4 to 6. These are the so-called S-N diagram obtained at R=0.05, -1 and 20. Fundamentally, open-hole tension-tension fatigue is reinforcement fiber-dominant behavior, on the other hand, both tension-compression and compression-compression fatigue behavior is controlled by both matrix resin and delamination properties.

Tension-tension (R=0.05)

Figure 4 shows that G40-800/5260 with a higher static strength level has a good open-hole tension-tension fatigue strength. There is a knee point in S-N diagram for both G40-800/5260 and IM600/PIXA-M. It is due to the failure mode transition from static to fatigue failure mode. IM600/PIXA-M has a steeper sloop and lowest tension-tension fatigue strength. On the other hand, in a case of MR50K/PETI-5, specimen was run-out at 97.5% level of static open-hole tension (OHT) strength, and there is little fatigue degradation up to $5x10^6$ cycles. S-N curve is flat as shown by the dotted line and the engineering fatigue endurance limit determined at 10^7 cycles is kept over 95% of OHT. MR50K/PETI-5 has a good retention of static open-hole tension strength to room temperature tension-tension fatigue strength.

Tension-compression (R= -1)

It is found from Fig. 5 that G40-800/5260 with a higher open-hole compression (OHC) strength has a better room temperature fully reversed tension-compression fatigue strength, and every fully reversed tension-compression fatigue lives are lowest as compared with tension-tension and compression-compression fatigue lives shown in Figs. 4 and 6. And it is clearly recognized the existence of the knee point around $4x10^4$ cycles, in particular in a case of IM600/PIXA-M and the S-N curve can be expressed by the two-straight line. This is identical to the results of macroscopic fracture examinations. There is a distinct transition in fatigue failure appearance from compressive- to tensile failure mode as shown in Fig. 10 [3]. In a lower cycles region than the knee point ($\leqq 4x10^4$ cycles), fatigue fracture appearance revealed a crushing mode of failure along a section transverse to the load axis and passing through the hole. It is almost same to compression-compression fatigue. In a higher cycles range, many$\pm 45^\circ$ plies sheared out of the surrounding 90° plies, creating a large delaminated surface in the process. Fibers in 0° plies failed along the underlying 45° transverse fracture line in the vicinity of the hole. Father away from the hole, the 0° plies usually fractured more uniformly perpendicular to the load axis. It is fundamentally corresponded to those for tension-tension fatigue except for the amount of creating a large delaminated zone and fracture manner of 0° plies.

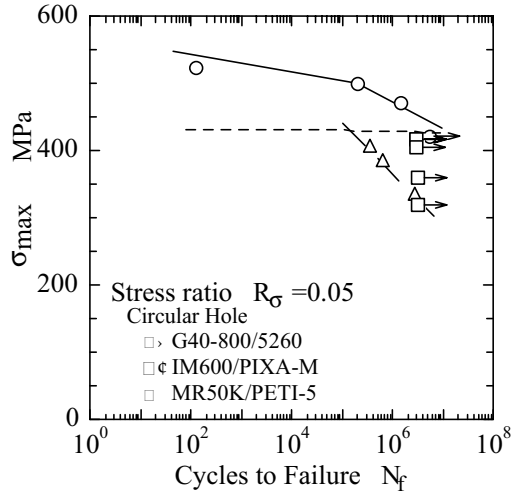

Fig. 4 S-N diagram for R=0.05

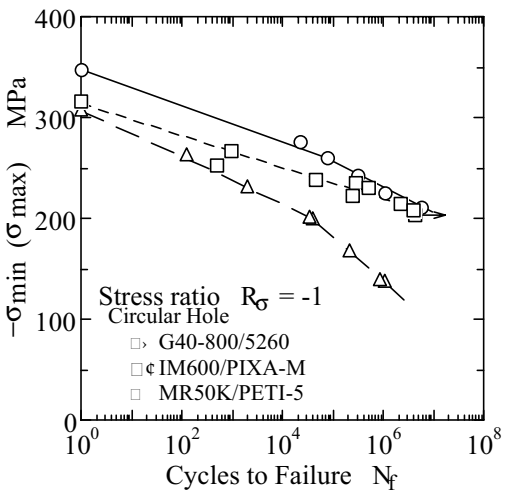

Fig. 5 S-N diagram for R= -1

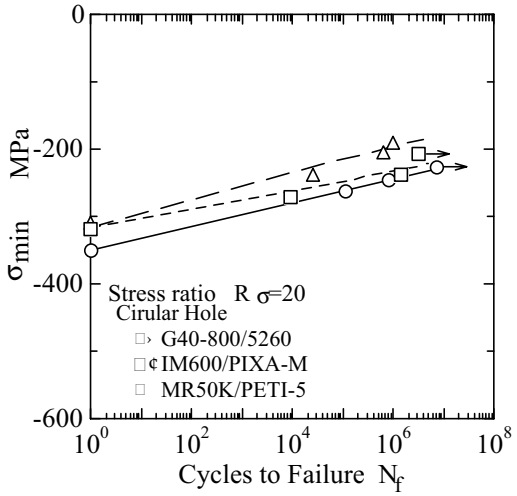

Fig. 6 S-N diagram for R=20

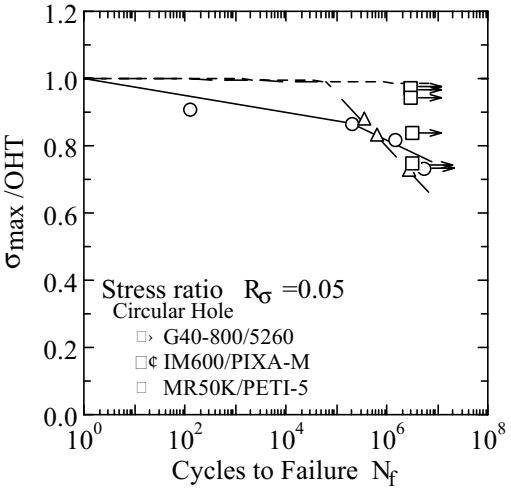

Fig. 7 Normalized S-N diagram for R=0.05

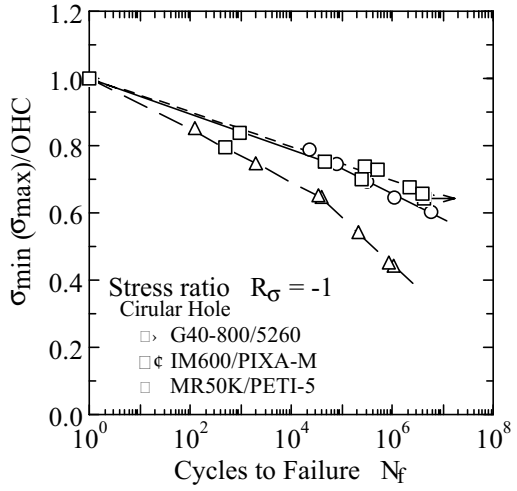

Fig. 8 Normalized S-N diagram for R= -1

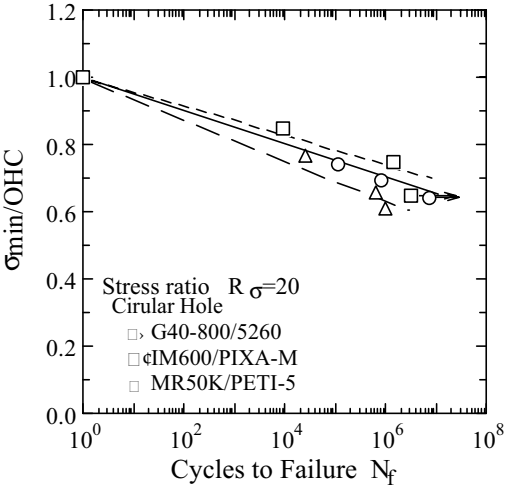

Fig. 9 Normalized S-N diagram for R=20